PROFOZ README File

1. Overview

This document provides a brief description of the OMI PROFOZ product. PROFOZ contains the retrieved ozone profile, a priori ozone profile and a prior error, total, stratospheric, and tropospheric ozone columns (TO, SOC, TOC), other retrieved auxiliary parameters, random-noise and total retrieval errors for all of the retrieved quantities, the retrieval Averaging Kernels (AKs) for the ozone profile, and the random-noise measurement error covariance matrix for ozone. In addition, it contains other ancillary information produced from the PROFOZ algorithm applied to OMI "global mode" measurements. In the global mode each file contains a single orbit of data. In each orbit, OMI measurements cover approximately 2600 km wide cross-track swath from pole to pole (sunlit portions only). Currently, PROFOZ products are not produced when OMI goes into the "zoom mode," which occurs for one day every 32 days.

The ozone profile is output in partial ozone columns (DU) for a 24-layer (25 level) atmosphere. The vertical grid varies from pixel to pixel in the lower stratosphere and troposphere, but is fixed at higher altitudes. The 25-level vertical pressure grid is set initially at $P_i = 2^{-i/2}$ atm for i = 0, 23 and $P_{24} = 0$. This pressure grid is then modified: The daily NCEP thermal tropopause pressure is used to replace the level closest to it, and layers between surface and tropopause are distributed equally in logarithmic pressure. In addition to TO, SOC and TOC and corresponding errors are integrated from the profile and error covariance matrices. Note that the primary purpose of adjusting the model layering to tropopause height is to derive SOC and TOC; the actual value of the tropopause pressure has negligible effect on the retrieved TO and values at layers not affected by the layer adjustment. TOC and SOC can be re-calculated from the retrievals through interpolation if a different tropopause is available.

The partial ozone column $O_{3,i}$ can be converted to mean mixing ratio $O_{3,i}$ (ppbv) at each layer using the following formula (assuming ozone is well mixed in that layer):

$$O_{3,i}\ (\text{ppbv}) = 1.251 \times O_{3,i}\ (\text{DU}) / (P_{i+1} - P_i) \times 1013.25 \times (R / (R + Z_{\text{mid},\,i}))^2,$$

where P_{i+1}, P_i are the pressures in hPa at the two levels bounding layer i, R is the radius of the earth, and $Z_{\text{mid},i}$ is the center altitude of that layer. This formula is accurate to better than 1%. Similarly, TOC can be converted to mean mixing ratio by using tropopause and surface pressure. Using mixing ratios has certain advantages over using TOCs by reducing the variability due solely to the tropopause and surface pressure.

The retrievals are time-consuming due to on-line radiative transfer calculations. We co-add 4 pixels along-track to speed up processing, which can also reduce the retrieval noise. No pixels are skipped: The OMI global coverage is maintained. Thus, the spatial resolution at nadir is 52 km (along-track) × 48 km (across-track), and coarser at off-nadir swath positions.

2. Algorithm Description

Ozone profiles are retrieved from OMI UV radiances (270-330 nm) using the optimal estimation technique and using the vector linearized discrete ordinate radiative transfer model (VLIDORT)

[Spurr, 2006] to simulate radiances and weighting functions. The algorithm has been described in detail in Liu et al. [2010a]. The spectral region covers both OMI UV1 (270-309 nm) and UV2 (312-330 nm) channels. Due to different channel spatial resolutions, two UV2 pixels are co-added across the track. Validation of OMI radiances shows systematic wavelength and across-track position dependent errors. A first-order correction, derived using two days of zonal mean MLS data (above 215 hPa) and climatological ozone (below 215 hPa) in the tropics, is applied to OMI radiances before the retrieval process independent of latitude and time [Liu et al., 2010a].

Because the retrieval problem is ill-posed, the retrievals are constrained and stabilized using the a priori ozone profile climatology by McPeters et al. [2007] and OMI random-noise measurement errors. The McPeters climatology, derived from 15 years of ozonesonde and SAGE data, provides monthly and zonal mean ozone profiles and standard deviations at 61 levels from 0 to 60 km. To avoid discontinuities, the climatology is interpolated as a function of latitude and time for a given latitude and date. The standard deviations are used to construct the diagonal values of the a priori covariance matrix, and a correlation length of 6 km is used to construct the off-diagonal elements.

Radiance calculations are made for Rayleigh atmospheres (no aerosols) with Lambertian reflectance assumed for surface and for clouds. The surface albedo is initialized from a database [Kleipool et al., 2008]. Clouds are taken to be at the Optical Centroid Pressure (OCP) from the OMI Raman cloud product [Joiner and Vasilkov, 2006]. Only cloud pressure values meeting all the recommended quality flags are used. Pixels without good quality OCP values are filled in by spatial interpolation on an orbital basis. Remaining empty values after the interpolation are filled in by a climatology derived from several years of OMI OCPs. An effective cloud fraction is initially determined from the radiance at ~347 nm. Both surface albedo and cloud fraction are also retrieved as auxiliary parameters. Partial cloudy scenes are treated using the mixed Lambertian model assuming a cloud albedo of 0.80. When the cloud fraction is derived to be greater than 1, the cloud fraction is set to 1 and a cloud albedo is derived. To account for the temperature dependence of ozone absorption, we use the daily NCEP reanalysis temperature profiles. Ozone cross sections are from Malicet et al. [2005], as this dataset delivers the best ozone profile retrieval performance [Liu et al., 2007; C. Liu et al., 2013]. In our retrievals, aerosols, clouds, and surface pressure are either not accurately known or are not modeled in the retrievals. In addition, the absolute values of OMI radiances may still contain small biases even though they are well calibrated. We thus fit wavelength-dependent surface albedo values (zero order for UV-1, first-order polynomial for UV-2) as tuning parameters to partly account for these effects.

Several changes have been made in the production of the current PROFOZ product since the version of Liu et al. [2010a], as described in Section 2.1 of Kim et al. [2013]. But the changes are not significant except for high-latitude winter and spring, i.e., large solar zenith angles (SZA), where the results become worse (see section 4.2 in Data Quality Assessment). The changes are:

a. Radiative transfer calculations and spectral co-adding

To speed up calculations, the previous version used effective ozone cross sections convolved by slit functions and weighted by solar irradiance spectra, in 6-stream VLIDORT calculations. Five spectral pixels were co-added in UV-1 and two in UV-2, to further speed up calculations. In the

current version, radiative transfer calculations are done more accurately, with 8 streams at selected wavelengths (~90 wavelengths) and then are interpolated to a fine spectral grid (every 0.05 nm) using weighting functions. The radiances and weighting functions are then convolved by OMI slit functions and interpolated to the OMI wavelength grid. No spectral co-adding is used in the current version.

b. Radiometric calibration

The empirical soft calibration is re-derived to be consistent with the improved radiative transfer calculations described above, using the approach described in Liu et al. [2001a].

c. Measurement errors

The use of measurement errors in the optimal estimation scheme has a large impact on the retrievals. In Liu et al. [2010a], random-noise errors from OMI level 1b (L1B) data are used. But those error estimates in OMI L1B are overestimated by the square root of co-additions (2, 4, and 5 for arctic, mid-latitude, and tropical measurements, respectively) [Braak, 2010]. However, using the correct random error estimates would actually significantly degrade the retrievals, probably because other additional errors are not included. Therefore we impose a minimum error of 0.4% in UV-1 and 0.2% in UV-2 (if the random-noise errors are smaller than these values) to account for total errors.

d. Cloud product and surface albedo database

We switched to using the OMI Raman cloud product [Joiner and Vasilkov, 2006] instead of the OMI O_2-O_2 cloud product [Acarreta et al., 2004]. We now use the OMI surface albedo database [Kleipool et al., 2008] instead of the previous TOMS-derived database [Liu et al., 2010a].

e. Fitting parameters

Several changes have been made to the selection of fitting parameters compared to the version of Liu et al. [2010a]. Previously, we fit a first-order polynomial in each channel for wavelength shift between radiance/ozone cross sections, partly accounting for some artifact shifts resulting from the spectral co-adding. Since we do not use spectral co-adding in this version, we only fit a zero-order shift for each channel. In addition, we add a parameter to fit the vertical column density of BrO and fit an additive offset for UV-1 to partly account for stray-light errors.

3. Data Quality Assessment

The previous version of retrievals have been validated against Aura MLS stratospheric ozone profiles and SOC [Liu et al., 2010b], ozonesonde observations [Zhang et al., 2010; Wang et al., 2011; Lal et al., 2013], GEOS-Chem and TES tropospheric ozone [Zhang et al., 2010], aircraft measurements of ozone in the Upper Troposphere and Lower Stratosphere (UTLS) [Pittman et al., 2009], and various OMI/MLS TOC. For this version, the retrieved total ozone has been compared with OMI operational products and ground-based Brewer measurements [Bak et al., 2014], and the retrieved tropospheric ozone column has been compared with other OMI tropospheric ozone products and ozonesonde observations [Ziemke et al., 2014].

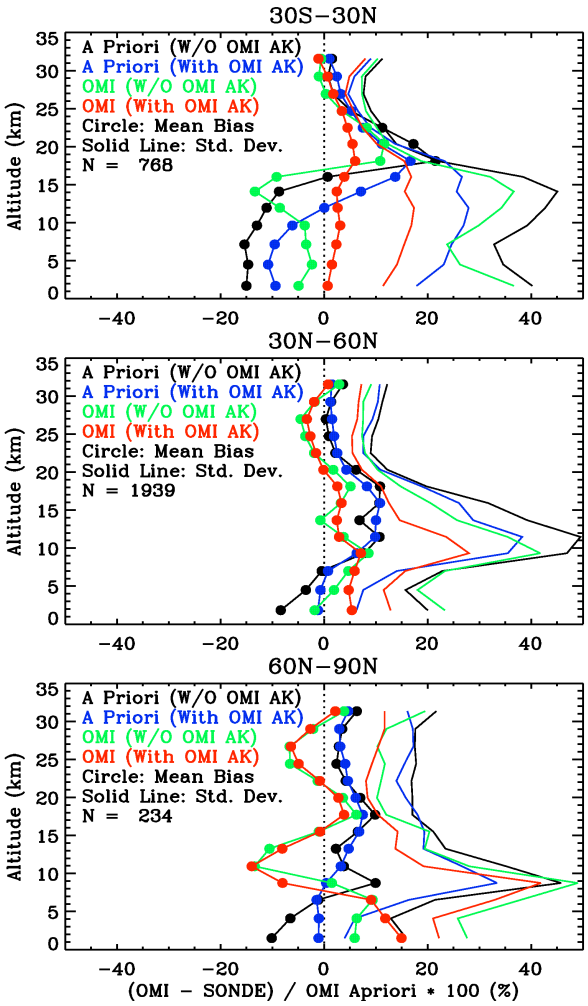

Figure 1 Comparison of ozone profiles between OMI, OMI a priori, and ozonesondes for 3 latitude regions during October 2004-February 2008. OMI and sonde data are within 12 hours and the OMI pixel overpasses the sonde station. Only OMI pixels with effective cloud fraction less than 0.30 and UV-1 across-track positions 4-27, SZA<75° are used. "W/O OMI AK" means that OMI averaging kernels (AKs) are not applied to ozonesonde data and "With OMI AK" means that OMI AKs are applied.

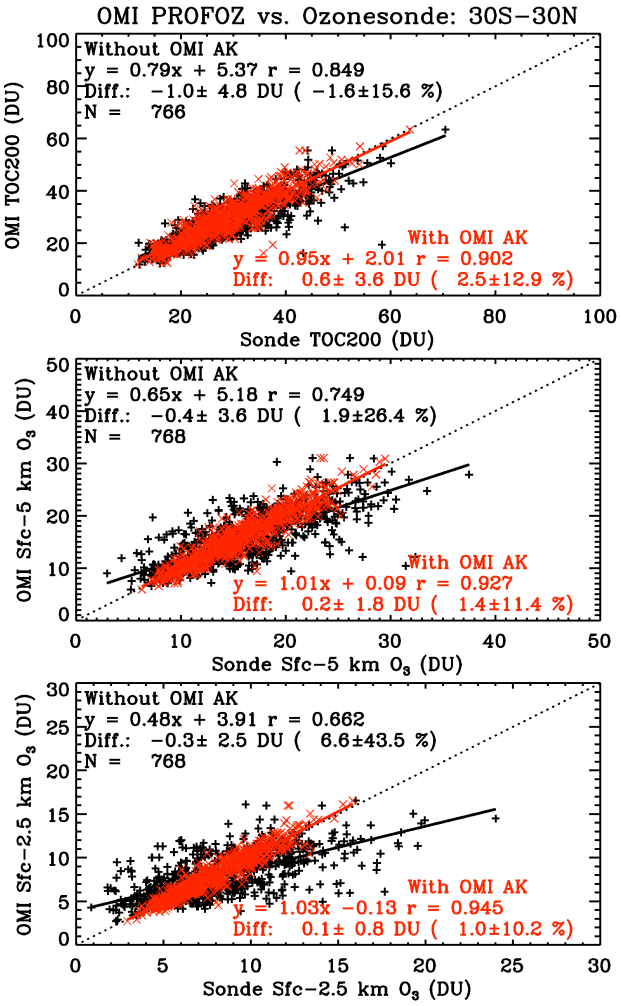

Figure 2 Comparison of TOC for surface-200 hPa, surface~5 km (first 2 retrieval layers), and surface~2.5 km (first retrieval layer) between OMI and ozonesondes in the tropics (30°S-30°N) during October 2004-February 2008. The solid line is the linear regression. The linear regression slope and intercept, correlation coefficient, absolute and relative mean biases and standard deviations are shown. Black is for original ozonesonde data and red for ozonesonde data convolved with OMI AKs.

3.1 Validation against MLS data

We have validated previous version of ozone profiles between 0.22-215 hPa and SOC down to 215 hPa against MLS v2.2 data from 2006. The global mean biases are within 2.5% above 100 hPa and 5-10% below 100 hPa; the standard deviations of the differences (1σ) are 3.5-5%

between 1-50 hPa, 6-9% above 1 hPa and 8-15% below 50 hPa. OMI SOC shows a small bias of –0.6% with a standard deviation of 2.8%. The validation demonstrates that SOC can be derived accurately from OMI alone, with errors comparable or even smaller than those from current MLS retrievals, and it demonstrates implicitly that TOC can be retrieved accurately from OMI alone. The excellent agreement with MLS data shows that OMI retrievals can be used to augment the validation of MLS and other stratospheric ozone measurements made with even higher vertical resolution. See Liu et al. [2010b] for more detail.

3.2 Validation against ozonesonde data (unpublished)

We have validated this version of ozone profiles and several tropospheric partial ozone columns against collocated ozonesonde observations in the northern hemisphere during August 2004-February 2008. The collocation criteria are: within 12 hours, and OMI footprint overpasses the ozonesonde station. We only use pixels with effective cloud fraction < 0.3, across-track positions between 4-27, SZA < 75º and fitting root mean square (RMS, RMS of ratio of fitting residuals to assumed measurement error) < 2.0.

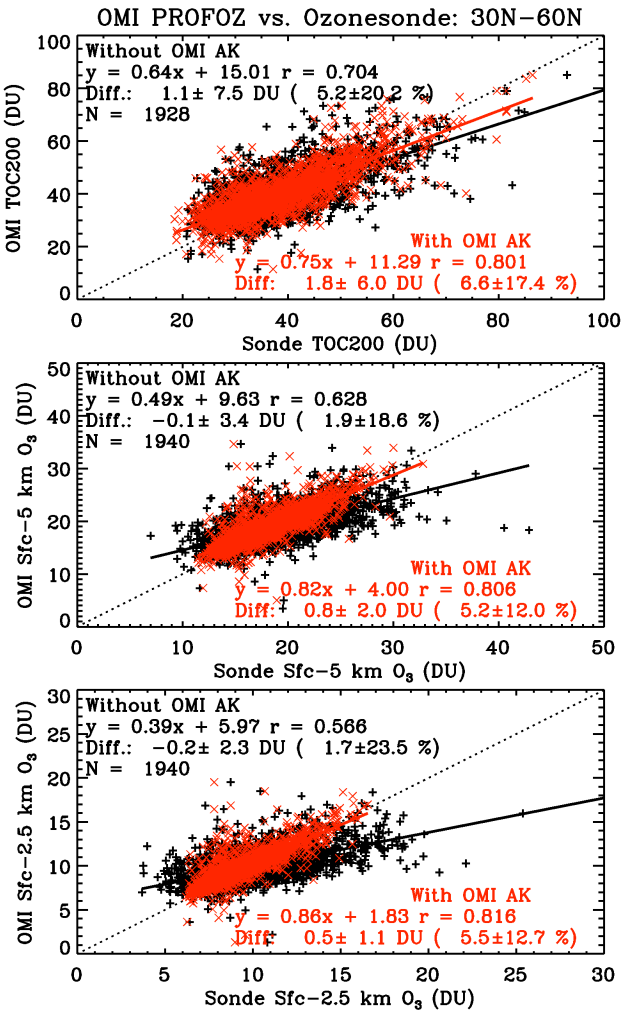

Figure 3 Same as **Figure 2** but for northern middle latitudes (30°N-60°N).

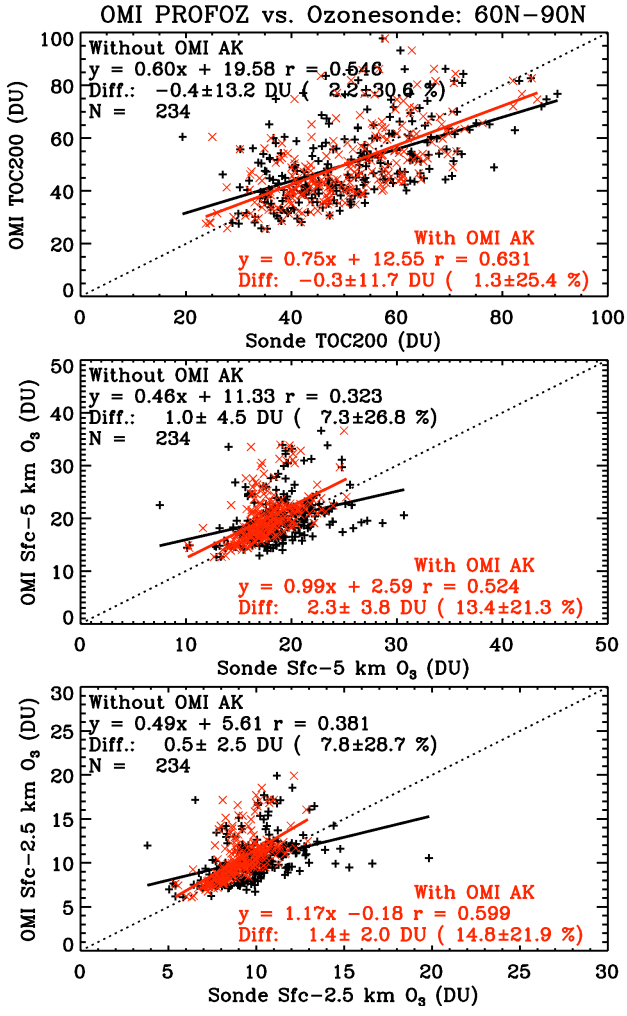

Figure 4 Same as **Figure 2** but for northern high latitudes (60°N-90°N).

Figure 1 summarizes the profile comparison for three latitude regions. With OMI AKs, the mean biases are within 10% in the tropics and mid-latitudes, and are within 15% at high latitudes. The OMI mean biases are larger than OMI a priori biases at high latitudes. At middle and high latitudes, the tropospheric mean biases vary with seasons. For middle latitudes, the tropospheric mean biases range from 0%−-5% (from layer 1 to 4 above the surface) during the summer to 10−20% during the winter. For high latitudes, the tropospheric means biases range from 5%−-36% during the summer and 25−-15% during the spring. The standard deviations in the troposphere are within 15% in the tropics and within 25% (up to 18% during the summer and to 33% during the winter) in the middle latitudes. For high latitudes, standard deviations in the troposphere are 20-40% (all seasons), ranging from 16−22% in the summer to 25−45% during the spring.

Figures 2-4 summarize the comparisons of partial ozone columns (surface-200 hPa, surface~5 km, surface~2.5 km) with ozonesonde data for the three respective latitude regions. Without OMI AKs, the mean biases for surface-200 hPa are within 1.1 DU for different latitude regions, but ranging from -2 DU during the summer to 4.2 DU during the winter for middle latitudes, and from -9.4 during the summer to 5 DU during the winter for high latitudes; the standard deviations are 4.8 DU, 7.4 DU (from 5.9 DU during the summer and fall to 8.3 DU during the spring), and 12.9 DU (from 6.4 DU during the fall to 14.6 DU during the spring) for the three latitude regions, respectively. The correlation and slope decrease with increasing latitude (SZA) due to decreasing sensitivity. The correlation and slope also decrease deeper into the lower troposphere due to reduced sensitivity to ozone at lower altitudes. The slope is less than 1 due to both reduced sensitivity at lower altitudes and the strong a priori constraint. With OMI AKs applied to ozonesonde data, the changes in mean biases are small, mostly within 1 DU (within 2 DU for surface-200 hPa ozone columns during a few seasons), but the correlation, slope, and standard deviation are significantly improved.

3.3 Total Ozone Validation

The integrated TO from our retrievals has been compared with ground-base Brewer measurements and the OMIO3, OMDOAO3, OMO3PR operational products from 2005 through 2008 [Bak et al., 2014]. Excellent agreement is observed between our integrated and Brewer total ozone, with a mean difference of less than ±1% at most individual stations. In addition, the total ozone is found to have insignificant dependence on viewing geometry, cloud parameters, total ozone column. Furthermore, the difference against Brewer total ozone shows no apparent long-term drift and seasonality.

3.4 Known issues

a. Latitudinal and seasonal dependent biases

As we can see from the validation against ozonesonde observations, there are seasonally- and latitudinally-dependent mean biases in our retrievals, which are different from those in the a priori. This is likely due to inadequate radiometric calibration especially with respect to errors depending on signal (e.g., stray-light) and forward model simulations. In addition, the assumed measurement errors in level 1b data can also cause seasonal/latitudinal dependent biases (see section 3). In addition, relatively limited amount of information in the troposphere and inadequate a prior constraint also contribute to this latitudinal and seasonal dependent biases. It

has been shown that the use of an improved tropopause-based ozone profile climatology can better constrain the ozone profile retrievals and significantly reduce the latitudinal and seasonal dependent biases [Bak et al., 2013].

b. Cross-track dependent biases

Despite of the empirical soft calibration to correct for cross-track dependent biases, cross-track dependent biases are still visible from the data. To further remove the cross-track striping, the striping patterns can be derived as a function of cross-track positions and latitude using retrievals; it is recommended to use at least 5-7 days of data to reduce the impact of ozone variability on the striping patterns.

c. Retrievals at large solar zenith angles

Currently, retrieved TOC at high SZA > 75º during the winter and spring shows large biases, of ~10 DU relative to ozonesonde observations. The standard deviations are also large. Some of the poor performance is caused by the change in the assumed measurement errors from the previous version, which changes the mean biases from ~-6 DU to ~10 DU, and also significantly increases the standard deviations from ~9 DU to ~16 DU. It has been shown that the use of an improved tropopause-based ozone profile climatology can better constrain the ozone profile retrievals and significantly reduce the large positive biases in TOC at high latitudes [Bak et al., 2013].

d. Ozone hole conditions

Retrievals often fail due to large negative ozone values at some layers under ozone hole conditions. This is not caused by the ozone profile climatology used, because using a total ozone-dependent climatology (e.g., TOMS climatology) does not solve this issue. Using UV2 only can actually significantly reduce the rate of retrieval failure. We noticed that the observed radiances are much larger than the simulated radiances at shorter wavelengths. We suspect that some of the large discrepancies might be related to the presence of polar stratospheric clouds, which significantly enhance the radiances at shorter wavelengths. Although fitting a multiplication polynomial in UV-1 (as done in our GOME retrievals) or using a logarithmic state vector can improve the rate of retrieval success, we are not currently considering these options because the former will lose measurement information elsewhere and the latter can cause larger biases in the troposphere for other regions.

4. Product description

The PROFOZ product is written as an HDF-EOS5 swath file. For a list of tools that read HDF-EOS5 data files, please visit these links:
http://disc.gsfc.nasa.gov/Aura/tools.shtml
http://hdfeos.net/

A single file is for a swath (i.e., orbit) of OMI retrievals over the sun-lit portion of the orbit. Because of spatial co-adding, each swath contains about ~400 pixels along-the-track and 30 pixels across-the-track (UV1). Each file is ~24 MB. All the files are ordered in time. The information provided in the file includes 13 geo-location fields and 45 data fields. For a complete list of the fields, flags, and their interpretation please read the file specification.

The geo-location fields include center longitude and latitude, approximate corner longitude and

latitude, solar, viewing and relative azimuthal angles, time, spacecraft longitude, latitude, and altitude, and ground pixel quality flags from level 1b data. The corner longitudes and latitudes are derived by assuming no pixel overlap and gap; only the variation of spatial resolution vs. across-track position is considered. The viewing geometry is defined for the whole pixel, by averaging the left edge, center, and the right edge viewing geometry.

The data fields include the information for all the variables in the state vector (including retrieved value, initial value, a priori error, precision, and solution error), the derived TO, SCO, and TCO and associated precision and solution error, atmospheric profiles of pressure, altitude, and temperature and index to the level of tropopause, retrieval characterization (retrieval AKs for O_3, information content, noise correlation matrix for O_3), quality flags (measurement quality flags from level 1b data, averaging fitting residuals in radiances and average fitting RMS for each channel and the whole spectral region, exit status, number of iterations), aerosol/cloud/surface albedo information (aerosol index derived from 1st-order wavelength-dependent surface albedo, glint probability based on viewing geometry for water surface, effective cloud fraction, optical centroid pressure, and the number of wavelengths used in each channel and the number of OMI small number of pixels. To reduce the file size, AKs and O_3 noise correlation matrix are scaled by 10000 to integers. Only the upper half off-diagonal elements are saved for O_3 noise correlation matrix. The O_3 random-noise covariance matrix, needed in data assimilation, can be derived from the noise correlation matrix and the retrieval precision for each layer. The Exit Status (ES) is one of the most important variables needed to assess the data quality. It is recommended to use $0 < ES < 10$. Other useful parameters that can be used to assess the retrieval quality include the fitting RMS, fitting residuals, cloud fraction, aerosol index, and glint probability. It is recommended to use retrievals with RMS <2.0 and average fitting residuals <2% (filter ~4% of the retrievals for SZA < 75º and 8% of the retrievals for larger SZA). As the fitting RMS typically varies with solar zenith angle and increases with time, it is even better to derive RMS thresholds for filtering data as a function solar zenith angle and time.

Currently, the data are only available in level 2 data format at AURA AVDC. The developers have a tool to grid the data to a standard grid (with evenly spaced longitude or latitude coordinates) and save the gridded data in IDL save/xdr format, and have generated daily and monthly gridded data at 1° longitude × 1° latitude and 2.5° longitude × 2° latitude resolutions. For questions and comments related to the PROFOZ algorithm and data quality and interest in gridded data, please contact Xiong Liu.

Notes on Using Averaging Kernels

Let us denote **Averaging Kernels** as **A**, and use i for column and j for row (**IDL style**) then $A(i,j) = \frac{\partial x_j'}{\partial x_i}$ i.e., the sensitivity of retrieved partial ozone column (DU) at layer j to the change in ozone (DU) at layer i (from the a priori ozone column). AKs indicate retrieval sensitivity and the vertical resolution of retrievals. Note the AKs for different units (e.g., DU or ppbv) are different, the DU/DU does not cancel out because the conversion from DU to ppbv varies with altitude (e.g. resulting from different T, P).

When comparing with measurements/model simulations that have much better vertical resolution than our satellite retrievals, we can apply retrieval AKs to the high-resolution data so that we are comparing data at the same vertical resolution. The steps to apply AKs are:

- Convert/integrate/interpolate the high-resolution ozone profile to partial ozone columns at our retrieval altitude grid. In case the high-resolution profile does not cover the retrieval altitude range, augment the high-resolution profile (ozonesonde only up to ~35 km, SAGE only down to ~10-15 km) with other data (e.g., climatological profiles or even OMI retrievals).

- Apply retrieval AKs using:

$$X'_j = X_{a,j} + \sum_{i=1}^{nl} A(i,j) \times (X_{t,i} - X_{a,i})$$

Where X' is the high-resolution profile convolved with retrieval AKs, X_t is the high-resolution profile converted to the retrieval altitude grid and X_a is the a priori profile used in satellite retrievals.

References

Bak, J., X. Liu, J.C. Wei, L.L. Pan, K. Chance, and J.H. Kim (2013), Improvement of OMI ozone profile retrievals in the upper troposphere and lower stratosphere by the use of a tropopause-based ozone profile climatology, Atmos. Meas. Tech., 6, 2239-2254, doi:10.5194/amt-6-2239-2013.

Bak, J., X. Liu, J. H. Kim, K. Chance, and D. P. Haffner (2014), Validation of OMI Total Ozone Retrievals from the SAO Ozone Profile Algorithm and Three Operational Algorithms with Brewer Measurements, *Atmos. Chem. Phys. Discuss.*, 14, 4051-4087, doi:10.5194/acpd-14-4051-2014.

Braak, R. (2010): Bug fix for GDPS measurement noise calculation algorithm, KNMI, Technical Note, TN-OMIE-KNMI-935.

Joiner, J., and A. P. Vasilkov (2006), First results from the OMI rotational Raman scattering cloud pressure algorithm, *IEEE Trans. Geosci. Remote Sens.*, *44*, 1272-1282.

Kim, P. S., D. J. Jacob, X. Liu, J. X. Warner, K. Yang, K. Chance, K., V. Thouret, and P. Nedelec (2013), Global ozone–CO correlations from OMI and AIRS: constraints on tropospheric ozone sources , Atmos. Chem. Phys., 13, 9321-9335, doi:10.5194/acp-13-9321-2013.

Kleipool, Q. L., M. R. Dobber, J. F. de Haan, and P. F. Levelt (2008), Earth surface reflectance climatology from 3 years of OMI data, *J. Geophys. Res.*, *113*, 18308, doi: 10.1029/2008JD010290.

Lal, S., S. Venkataramani, S. Srivastava, S. Gupta, C. Mallik, M. Naja, T. Sarangi, Y. B. Acharya and X. Liu (2013), Transport effects on the vertical distribution of tropospheric ozone over the tropical marine regions surrounding India, J. Geophys. Res. Atmos., 118, 1513–1524, doi:10.1002/jgrd.50180.

Liu., C., X. Liu, K. Chance (2013), The impact of using different ozone cross sections on ozone profile retrievals from OMI UV Measurements, *JQSRT*, 10.1016/j.jqsrt.2013.06.006.

Liu, X., P. K. Bhartia, K. Chance, R. J. D. Spurr, and T. P. Kurosu (2010a), Ozone profile retrievals from the Ozone Monitoring Instrument, *Atmos. Chem. Phys.*, *10*, 2521-2537.

Liu, X., P. K. Bhartia, K. Chance, L. Froidevaux, R. J. D. Spurr, and T. P. Kurosu (2010b), Validation of Ozone Monitoring Instrument (OMI) ozone profiles and stratospheric ozone columns with Microwave Limb Sounder (MLS) measurements, *Atmos. Chem. Phys.*, *10*, 2539-2549.

Liu, X., K. Chance, C.E. Sioris, and T.P Kurosu (2007), Impact of using different ozone cross sections on ozone profile retrievals from Global Ozone Monitoring Experiment (GOME) ultraviolet measurements, *Atmos. Chem. Phys.*, 7, 3571-3578.

Liu, X., et al. (2005), Ozone profile and tropospheric ozone retrievals from Global Ozone Monitoring Experiment: Algorithm description and validation, *J. Geophys. Res.*, *110*, D20307, doi:10.1029/2005JD006240.

Malicet, C., D. Daumont, J. Charbonnier, C. Parisse, A. Chakir, and J. Brion (1995), Ozone UV spectroscopy, II. Absorption cross-sections and temperature dependence, *J. Atmos. Chem.*, *21*, 263-273.

McPeters, R. D., G. J. Labow, and J. A. Logan (2007), Ozone climatological profiles for satellite retrieval algorithms, *J. Geophys. Res.*, *112*, D05308, doi:10.1029/2005JD006823.

Pittman, J. V., et al. (2009), Evaluation of AIRS, IASI, and OMI ozone profile retrievals in the extratropical tropopause region using in situ aircraft measurements, *J. Geophys. Res.*, *114*, 24109, doi: 10.1029/2009JD012493.

Spurr, R. J. D. (2006), VLIDORT: A linearized pseudo-spherical vector discrete ordinate radiative transfer code for forward model and retrieval studies in multilayer multiple scattering media, *J. Quant. Spectrosc. Radiat. Transfer*, *102*, 316-342.

Wang, L., M.J. Newchurch, A.P. Biazoor, X. Liu, S. Kuang, M. Khan (2011), Evaluating AURA/OMI ozone profile retrievals using ozonesonde data and EPA surface measurements for August 2006, Atmos. Environ., 45, 5523-5530.

Zhang, L., Jacob, D. J., Liu, X., Logan, J. A., Chance, K., Eldering, A., and Bojkov, B. R., Intercomparison methods for satellite measurements of atmospheric composition: application to tropospheric ozone from TES and OMI, Atmos. Chem. Phys., 10, 4725-4739, doi:10.5194/acp-10-4725-2010, 2010.

Ziemke, J. R., et al. (2014), Assessment and applications of NASA ozone data products derived from Aura OMI/MLS satellite measurements in context of the GMI chemical transport model, *J. Geophys. Res. Atmos.*, 119, doi:10.1002/2013JD020914.